THE JOURNAL OF PHYSICAL CHEMISTRY B

Article

pubs.acs.org/JPCB

Relationship between Microviscosity and High-Frequency Viscosity of Polymer Gel Electrolytes

Tsuyoshi Yamaguchi,* Ryo Matsui, and Shinobu Koda

Department of Molecular Design and Engineering, Graduate School of Engineering, Nagoya University, Furo-cho, Chikusa, Nagoya, Aichi 464-8603, Japan

ABSTRACT: The frequency-dependent viscosity and conductivity of polymer gel electrolytes are investigated in the megahertz region to clarify how polymer affects the ionic mobility. The electric conductivity shows no dispersion below 10 MHz, where slow dynamics of polymer are observed in shear relaxation spectra, which indicates that the ionic motion is uncorrelated with the slow dynamics of polymers that determines the steady state shear viscosity. On the other hand, the shear viscosity around 100 MHz is somewhat correlated with the direct-current (DC) molar conductivity, suggesting that the measurement of the high-frequency viscosity can be a probe of the so-called microviscosity associated with the mobility of an ion.

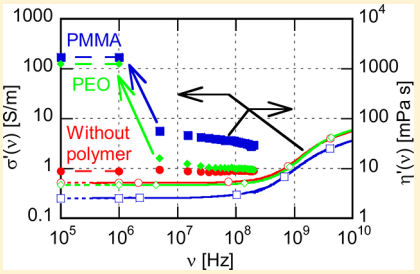

1. INTRODUCTION

Polymer gel electrolyte is a material composed of organic electrolyte and polymer dissolved in it. Because it can realize high ionic conductivity of organic electrolyte and high viscosity of polymer solution at the same time, it has been employed as an electrolyte of electrochemical devices such as lithium ion battery.[1,2]

The ionic conductivity and shear viscosity are usually correlated with each other through the Walden law, which states that the molar ionic conductivity is reciprocally proportional to the shear viscosity.[3,4] The advantage of the polymer gel electrolyte described above is thus regarded as the violation of the Walden law, which requires a specific explanation.

The conventional idea on the mechanism of the ionic transport of polymer gel electrolyte is that the motion of ions is decoupled from the slow dynamics of polymer that determines the macroscopic shear viscosity,[5,6] and that an ion feels the "microviscosity" of the organic electrolyte around the ion.[7−10] However, the degree of the decoupling between the motions of polymer and ion is not clear, and the physical meanings of the microviscosity are ambiguous. The idea of microviscosity is sometimes used in an expedient way to account for ionic conductivity, and it can thus be said that the microviscosity is defined through the ionic conductivity.

Rheological measurement is one of the important tools to investigate the origin of the shear viscosity of soft matters. The shear viscosity is measured as the function of frequency in rheological studies. Since the frequency-dependent shear viscosity shows relaxations at frequencies characteristic to the microscopic motions that determine steady-state shear viscosity, we can infer the mechanism of steady-state shear viscosity from the relaxation frequency. Similarly, the electric conductivity of electrolyte solutions can be measured as the function of frequency, and the relaxation frequency provides us with information on the mechanism of ionic conduction.[11,12] The origin of the relationship between the steady-state shear viscosity and the direct-current (DC) ionic conductivity can be investigated with a comparison between the spectra of shear viscosity and electric conductivity.[13]

The purpose of this work is to clarify the relationship between the transport mechanisms of ions and momentum in polymer gel electrolytes through the relaxation measurement. Polymer solutions are known to exhibit relaxations of the shear viscosity in the kHz region,[14] which is ascribed to the large-scale motions of a polymer chain such as the Rouse-Zimm mode. In addition, entanglement of chains, if present in concentrated solutions, leads to relaxation at much lower frequencies. The coupling between the ionic mobility and slow motion of polymers is thus expected to appear as the dispersion of the ionic mobility in the sub-megahertz region. In addition, the shear viscosity at frequencies higher than the dynamics of polymers is, in principle, regarded as the viscosity of background solvent, although it can be affected by the dissolution of polymers.[15−17] It is thus interesting to see whether the high-frequency viscosity is related to the microviscosity defined in terms of the ionic mobility. The correlation between the translational or rotational diffusion coefficients and the high-frequency viscosity of polymer solutions was already demonstrated by Lodge and co-workers,[16,18,19] and our present work can be regarded as its extension to ionic mobility in polymer gel electrolytes.

2. EXPERIMENTAL SECTION

2.1. Samples. The system we mainly investigate is composed of lithium perchlorate ($LiClO_4$), propylene carbonate (PC) and polymethylmethacrylate (PMMA), which has

Received: April 3, 2013
Revised: May 20, 2013

   dx.doi.org/10.1021/jp4033172 | J. Phys. Chem. B XXXX, XXX, XXX−XXX

been studied as a model polymer gel electrolyte.[5−7,20] Hereafter we call this system Li-PMMA.

Four variations of the Li-PMMA system were also studied for comparison. The first one is the solution of PMMA in PC (hereafter called PC-PMMA) without $LiClO_4$. In the second one, Li-PEO, the PMMA was replaced with polyethylene oxide (PEO). In the third one, Li-MIB, the PMMA was replaced with methyl isobutyrate (MIB), which can be regarded as the monomer of PMMA terminated with two hydrogen atoms. The fourth one, TEA-PMMA, uses tetraethlyammonium perchlorate (TEA-ClO_4) as an electrolyte instead of $LiClO_4$.

In all the systems except for PC-PMMA one, the ratio of the salts to PC was fixed to 0.869 mol/kg-PC, which is equivalent to 1 mol/dm^3 in the case of PC solution of $LiClO_4$. The mass fraction of polymers, PMMA, PEO or MIB, was varied as 0, 5, 10, and 15 wt %. All the measurements were performed at 25 °C by flowing thermostatted water around the sample vessel. The temperature of the sample was confirmed to be 25.0 ± 0.1 °C by monitoring the temperature with a thermistor.

PC (Kishida Chemicals, lithium battery grade) was dried with molecular sieves 3A (Kishida Chemicals) prior to use. $LiClO_4$ (Kishida Chemicals, lithium battery grade) and TEA-ClO_4 (Tokyo Chemicals Industry, > 98.0%) were dried in vacuum overnight at 150 °C. PMMA (weight-averaged molecular weight, M_w = 75 000) and PEO (M_w = 100 000) were purchased from Scientific Polymer Products and used as received. MIB (Sigma-Aldrich, > 99%) was dried with 3A molecular sieves prior to use.

The densities of all the samples were determined with a vibrating tube densimeter (DMA60/602, Anton Paar) in order to calculate the molar concentration.

2.2. Conductometry. The DC conductivity was determined with a conductance bridge (Fuso, 362B) and a homemade conductance cell.[21] The electrodes of the conductance cell were covered with platinum black so as to reduce the effects of the electrode polarization. The conductivities were measured at five frequencies between 200 Hz and 5 kHz, and the values at 5 kHz were employed as the DC conductivity after confirming that the difference between the values at the five frequencies was negligible. The impedance between the two electrodes of the conductance cell was also measured with an LCR meter (ZM2371, NF corporation) between 1 Hz and 100 kHz, and it was confirmed that there was no dispersion between 1 and 200 Hz. Although diffusion-time dependence of the self-diffusion coefficients of solute molecules in polymer gels in the microsecond or millisecond domain was sometimes reported in literatures,[22−27] we did not observe the corresponding dispersion of the electric conductivity.

The alternating-current (AC) conductivity from 300 kHz to 20 GHz was determined with dielectric spectroscopy using two vector network analyzers (VNAs), which was described in detail elsewhere.[28] The measurement between 300 kHz and 200 MHz was performed with a homemade flat probe and a VNA (ZVL3/03, Rhode & Schwarz). The electrical impedance of the probe was determined from the complex reflection coefficient, $S_{11}(\nu)$, and the complex AC conductivity, $\sigma(\nu)$, was calculated from the electrical impedance by assuming the equivalent circuit described in ref 28. The parameters of the equivalent circuits were determined from the measurements of air, water, and aqueous solutions of NaCl from 1 to 100 mmol/dm^3.[29] The measurement between 200 MHz and 20 GHz was performed with a dielectric probe (HP85070B, Hewlett-Packard) and a VNA (HP8720D, Hewlett-Packard). The AC conductivity was calculated from $S_{11}(\nu)$ with the three-point calibration method.[30] The reference samples were air, PC,[31] and 1 mol/dm^3 aqueous solution of NaCl.[29]

2.3. Viscometry. The steady-state shear viscosity, η_0, was measured with conventional viscometers. An Ubberhode viscometer was applied to samples whose values of η_0 are smaller than 6 mPa s. The values of η_0 of other samples were determined with a rotational viscometer (VT-550, HAAKE) equipped with a coaxial cylindrical sensor or a cone−plate viscometer (RVDV-IPCP, Brookfield) equipped with a spindle CPE-40.

The frequency-dependent complex shear viscosity, $\eta(\nu)$, was determined with shear impedance spectroscopy, which is described in detail in the literatures.[21,32] The frequency range was from 5 to 205 MHz. Shear impedance spectroscopy is the application of the quartz crystal microbalance with a dissipation (QCM-D) technology to viscometry.[33] The frequency-dependent viscosity was measured through the changes in the peak frequency and the width of the resonance of the crystal before and after the contact with a sample liquid. The electric circuit to detect the resonance response of the crystal was the same as that used in our previous works.[21,28,32]

3. RESULTS AND DISCUSSION

Figure 1 shows the steady-state shear viscosity, η_0, and the molar DC conductivity, Λ_0, as functions of the concentration of

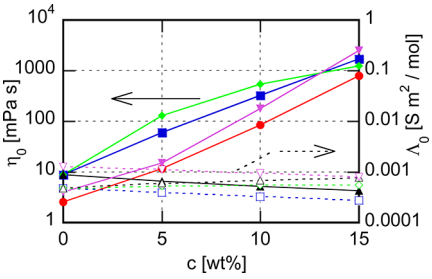

Figure 1. The steady-state shear viscosity, η_0 (filled symbols connected with solid lines, left axis), and the molar conductivity, Λ_0 (open symbols connected with dotted lines, right axis), are plotted as the functions of the concentration of polymers, *c*. The samples are PC-PMMA (red circles), Li-PMMA (blue squares), Li-PEO (green diamonds), Li-MIB (black upward triangles) and TEA-PMMA (purple downward triangles), respectively. The molar conductivity of PC-PMMA system is not plotted because it is not conductive.

the polymers. The steady-state shear viscosity increases with the addition of polymer, PMMA or PEO. The values of η_0 at the polymer concentration of 15 wt % are more than 100 times larger than the corresponding values without polymer. On the other hand, η_0 is lowered by the addition of the low molecular-weight cosolvent, MIB.

The molar DC conductivity, Λ_0, behaves quite differently from $1/\eta_0$ with the dissolution of polymers. PMMA decreases Λ_0 in both Li-PMMA and TEA-PMMA systems, although the amount of decrease, about 50% at c = 15 wt %, is far smaller than that of $1/\eta_0$. On the other hand, Λ_0 of the Li-PEO system is almost insensitive to the addition of PEO. The variations of Λ_0 in Li-PMMA and Li-PEO systems are in harmony with those reported in literatures on related systems. The conductivity of PC solution of $LiClO_4$ was reduced to about one-third with the addition of PMMA of M_w = 90000 at 15 wt

dx.doi.org/10.1021/jp4033172 | J. Phys. Chem. B XXXX, XXX, XXX−XXX

%.[7] Although their absolute value of Λ_0 without PMMA was a little smaller than ours, we consider it is probable due to the difference in the experimental method.[21] On the other hand, the addition of 10 wt % PEO to the solution of $LiCF_3SO_3$ in the mixture of PC and ethylene carbonate had little affect on the ionic conductivity.[9] In the Li-MIB system, Λ_0 increases with the concentration of MIB as is expected from the decrease in η_0.

Figure 2 exhibits the shear relaxation spectra, $\eta(\nu)$, of Li-PMMA systems. In the absence of PMMA, $\eta(\nu)$ shows no

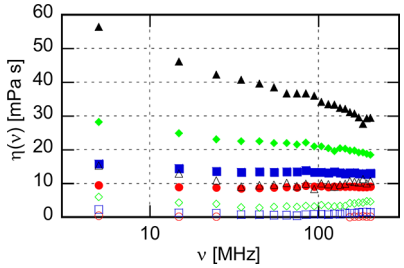

Figure 2. The shear relaxation spectra, $\eta(\nu)$, of Li-PMMA solutions are exhibited. The filled and open symbols denote the real and imaginary parts of $\eta(\nu)$, respectively. The concentrations of polymers are 0 wt % (red circles), 5 wt % (blue squares), 10 wt % (green diamonds), and 15 wt % (black triangles), respectively.

relaxation, and the value of the real part, $\eta'(\nu)$, agrees with the steady-state shear viscosity, η_0. Therefore, the value of η_0 of the solution without PMMA is determined by the dynamics faster than 200 MHz. The values of $\eta'(\nu)$ increase with the addition of PMMA. However, the amount of the increase is far smaller than that of η_0, and the absolute values of $\eta'(\nu)$ in the MHz region are far smaller than the corresponding values of η_0. It indicates that the steady-state shear viscosity is determined by the dynamics of polymer slower than 1 MHz. The variation of $\eta'(\nu)$ at 100 MHz with the concentration of PMMA is comparable with that of Λ_0, which supports the idea that the high-frequency viscosity has something to do with the microviscosity for the ionic mobility.

Both the real and imaginary parts of $\eta(\nu)$, denoted as $\eta'(\nu)$ and $\eta''(\nu)$, respectively, of polymer solutions decrease with increasing frequency in the frequency region below 40 MHz, which is ascribed to the high-frequency edge of the relaxation below 1 MHz associated with the slow polymer dynamics. In addition to the relaxation on the low-frequency side, another relaxation is observed in the 100 MHz region when the concentration of PMMA is high, and its relaxation frequency appears to decrease with increasing PMMA concentration.

The real part of the AC conductivity, $\sigma'(\nu)$, of Li-PMMA solutions is exhibited in Figure 3. Contrary to $\eta(\nu)$ shown in Figure 2, the AC conductivity below 10 MHz agrees well with the corresponding low-frequency limit, $\sigma_0 \equiv \sigma(0)$, determined with the conductance bridge. It clearly demonstrates that the slow dynamics of polymers below 1 MHz is uncorrelated with the translational motion of ions, as was proposed based on the comparison between Λ_0 and η_0. Although the decrease in Λ_0 with the dissolution of polymer is sometimes ascribed to the increase in η_0 of the solution,[34] the absence of the relaxation of $\sigma(\nu)$ below 10 MHz indicates that the decrease in Λ_0 results from the dynamics faster than 10 MHz.

There are two relaxations of $\sigma(\nu)$ shown in Figure 3. The largest one around 1 GHz is assigned to the reorientational

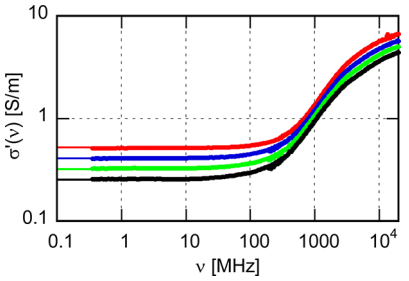

Figure 3. The real part of the AC conductivity, $\sigma'(\nu)$, of Li-PMMA solutions is plotted as a function of frequency. The filled symbols denote the AC conductivity, and the horizontal lines between 100 kHz and 1 MHz indicate the corresponding values of the DC conductivity determined with a conductance bridge. The concentrations of the polymer are, from upper to lower, 0 wt % (red), 5 wt % (blue), 10 wt % (green) and 15 wt % (black), respectively.

relaxation of PC. In addition, a small relaxation is observed above 100 MHz. We could not reproduce the spectra as the addition of the DC conductivity and the reorientational relaxation of PC, although we do not show the analysis for brevity. The relaxation frequency of the latter decreases with increasing the concentration of PMMA. The assignment of the relaxations of $\eta(\nu)$ and $\sigma(\nu)$ in the 100 MHz region are discussed after the introduction of the spectra of the PC-PMMA system.

The spectra of the shear viscosity and the AC conductivity of PC-PMMA solutions without salts are shown in Figures 4 and

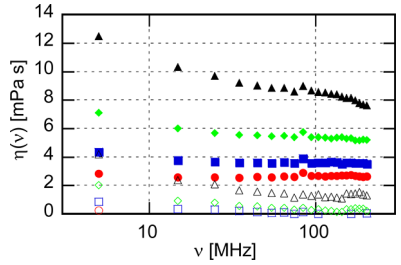

Figure 4. The shear relaxation spectra, $\eta(\nu)$, of PC-PMMA solutions are exhibited. The filled and open symbols denote the real and imaginary parts of $\eta(\nu)$, respectively. The concentrations of polymer are 0 wt % (red circles), 5 wt % (blue squares), 10 wt % (green diamonds), and 15 wt % (black triangles).

5, respectively. The shear relaxation spectra, $\eta(\nu)$, behave similarly with the addition of PMMA irrespective of the absence of $LiClO_4$, although the absolute values of the viscosity are

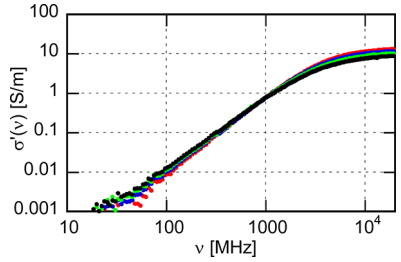

Figure 5. The real part of the AC conductivity, $\sigma'(\nu)$, of PC-PMMA solutions is plotted as a function of frequency. The concentrations of the polymer are, from upper to lower, 0 wt % (red), 5 wt % (blue), 10 wt % (green) and 15 wt % (black), respectively.

dx.doi.org/10.1021/jp4033172 | J. Phys. Chem. B XXXX, XXX, XXX–XXX

smaller. The two relaxations observed in Li-PMMA systems also appear in PC-PMMA ones. On the other hand, the conductivity spectra shown in Figure 5 are quite different from those of Li-PMMA solutions in Figure 3, which is partly because PC-PMMA solutions are not conductive in the low-frequency limit. In addition, no relaxation is observed around 100 MHz. Therefore, the relaxation of $\sigma'(\nu)$ of Li-PMMA systems in the 100 MHz region is not assigned to the dynamics of PMMA.

We have reported the relaxation spectra, $\eta(\nu)$ and $\sigma(\nu)$, of the solutions of $LiClO_4$ in PC at various concentrations in our previous work.[21] The relaxations of $\eta(\nu)$ and $\sigma(\nu)$ were observed in the 100 MHz region in cases of concentrated solutions, and the relaxation frequency decreased with increasing the concentration of the salt. The increase in η_0 and the decrease in Λ_0 with increasing the salt concentration were correlated with the slowing down of the relaxation around 100 MHz. Based on the observation above, we assigned the relaxation of $\eta(\nu)$ to the structural relaxation, and that of $\sigma(\nu)$ to the non-Markovian translational motion of ions due to the coupling with structural relaxation.

We consider that the relaxations in the 100 MHz region in the presence of PMMA are also associated with the structural relaxation. The structural relaxation of PC is retarded by the interaction with PMMA, which is directly reflected in the relaxation of $\eta(\nu)$ above 100 MHz. Since the retardation of the structural relaxation increases the viscosity of liquids in general, the retardation of the relaxation above 100 MHz can be the reason for the increase in $\eta'(\nu)$ in the megahertz region. The variation in the high-frequency viscosity by polymers is reported in the literature,[15−17] and it was ascribed to the modification of the dynamics of solvents around the polymer. The modified shear relaxation of solvents is also reported in these studies. Our assignment of the increase in $\eta'(\nu)$ in the megahertz region is thus in harmony with previous works. The translational motion of ions is affected by the retarded structural relaxation, leading to the dispersion of $\sigma(\nu)$ as is shown in Figure 3.

The viscosity at the frequency higher than the dynamics of polymer can be regarded in principle as the viscosity of the background solvent, as was described in the introduction. The increase in $\eta'(\nu)$ of Li-PMMA and PC-PMMA systems in the MHz region with increasing the PMMA concentration is thus interpreted as the increase in the viscosity of low molecular-weight liquids around polymer chains, PC solution of $LiClO_4$ and neat PC for Li-PMMA and PC-PMMA systems, respectively. If the decrease in Λ_0 with the dissolution of PMMA is caused by the coupling with the structural relaxation above 100 MHz that determines $\eta'(\nu)$ in the MHz region, it is natural that Λ_0 is correlated with $\eta'(\nu)$ in the MHz region, which may be regarded as the so-called microviscosity for the ionic mobility.

Figure 6 shows the shear relaxation spectra of Li-PEO solutions. The values of $\eta'(\nu)$ in the megahertz region are far smaller than the corresponding values of η_0 of Li-PEO solutions, and the high-frequency edge of the relaxation associated with slow polymer dynamics is observed on the low-frequency side, as is the case for PMMA solutions. However, the largest difference between the Li-PMMA and Li-PEO systems is in the dependence of $\eta'(\nu)$ around 100 MHz on the concentration of polymer. It is an increasing function of PMMA, while it increases little with the concentration of PEO. In addition, the relaxation above 100 MHz that appears in the

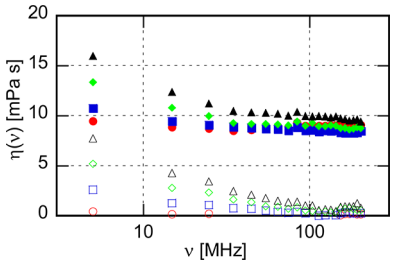

Figure 6. The shear relaxation spectra, $\eta(\nu)$, of Li-PEO solutions are exhibited. The filled and open symbols denote the real and imaginary parts of $\eta(\nu)$, respectively. The concentrations of polymers are 0 wt % (red circles), 5 wt % (blue squares), 10 wt % (green diamonds), and 15 wt % (black triangles).

Li-PMMA solutions is scarcely observed in Li-PEO solutions. We consider that the absence of the relaxation above 100 MHz is because PEO does not retard the structural relaxation of the PC solution of $LiClO_4$, and it is in harmony with the little change in $\eta'(\nu)$ around 100 MHz.

As was demonstrated in Figure 1, the dissolution of PEO hardly affects both the ionic mobility, Λ_0, and the high-frequency viscosity, $\eta'(\nu)$ around 100 MHz. It supports our idea that the reduction of Λ_0 in the Li-PMMA system is caused by the coupling with the structural relaxation in the 100 MHz region, which also enhances the high-frequency viscosity.

Figure 7 exhibits the $\sigma'(\nu)$ of Li-PEO solutions, which tells us the details of the ionic motion in these solutions. The

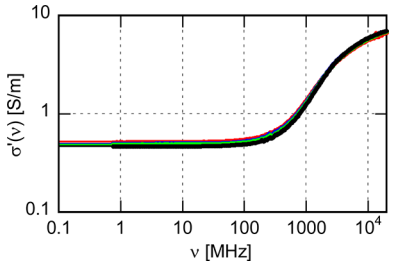

Figure 7. The real part of the AC conductivity, $\sigma'(\nu)$, of Li-PEO solutions is plotted as a function of frequency. The filled symbols denote the AC conductivity, and the horizontal lines between 100 kHz and 1 MHz indicate the corresponding values of the DC conductivity determined with a conductance bridge. The concentrations of the polymer are, from upper to lower, 0 wt % (red), 5 wt % (blue), 10 wt % (green) and 15 wt % (black), respectively.

conductivity spectra, $\sigma(\nu)$, show no relaxation below 10 MHz, and the values of $\sigma'(\nu)$ below 10 MHz agree with the corresponding values of DC conductivity, which indicates the decoupling between the slow polymer dynamics and the ionic motion also in the Li-PEO systems. Although one may expect strong direct interaction between Li^+ and PEO, it is not observed as the coupling between the ionic mobility and slow polymer motions. In addition, the low-frequency shift of the relaxation above 100 MHz was not observed, which is in harmony with the $\eta'(\nu)$ exhibited in Figure 6 and the small variation of Λ_0 with the dissolution of PEO.

The difference between Li-PMMA and Li-PEO systems is summarized as follows. The dissolution of PMMA retards the structural relaxation of the electrolyte solution between polymer chains, which increases $\eta'(\nu)$ in the megahertz region. The mobility of ions is reduced by the same structural relaxation, leading to the decrease in the molar DC

dx.doi.org/10.1021/jp4033172 | J. Phys. Chem. B XXXX, XXX, XXX−XXX

conductivity, Λ_0. On the other hand, PEO hardly affects the structural relaxation of the PC solution of $LiClO_4$, which explains why both the high-frequency viscosity and the DC molar conductivity are insensitive to the dissolution of PEO. We guess that the difference in the high-frequency viscosity of Li-PMMA and Li-PEO systems stems from that in the chain flexibility of the polymers. The motion of PC is retarded by the restricted segmental dynamics of PMMA, while the flexible segmental dynamics of PEO does not perturb the dynamics of PC.

Li^+ is a small cation, interacting with other molecules through strong Coulombic interaction. The direct interaction between polymer and ions may thus be a reason for the variation of the transport properties.[8,34,35] The ionic association between Li^+ and ClO_4^- may also be affected by the polymers,[8,36] which can explain the decrease in Λ_0 in the Li-PMMA system. Therefore, the behaviors of Li-PMMA and Li-PEO systems observed in this work may be specific to lithium salts. In order to examine such a possibility, the TEA-PMMA system is also studied, in which Li^+ is replaced with a bulky cation, TEA^+.

The frequency-dependent viscosity and conductivity of TEA-PMMA solutions are demonstrated in Figures 8 and 9,

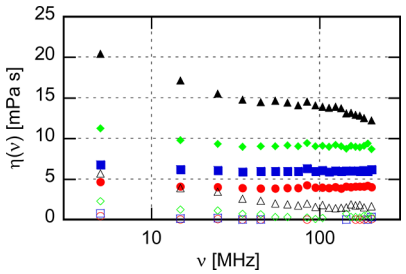

Figure 8. The shear relaxation spectra, $\eta(\nu)$, of TEA-PMMA solutions are exhibited. The filled and open symbols denote the real and imaginary parts of $\eta(\nu)$, respectively. The concentrations of polymers are 0 wt % (red circles), 5 wt % (blue squares), 10 wt % (green diamonds), and 15 wt % (black triangles).

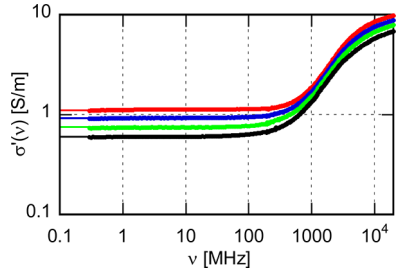

Figure 9. The real part of the AC conductivity, $\sigma'(\nu)$, of TEA-PMMA solutions is plotted as a function of frequency. The filled symbols denote the AC conductivity, and the horizontal lines between 100 kHz and 1 MHz indicate the corresponding values of the DC conductivity determined with a conductance bridge. The concentrations of the polymer are, from upper to lower, 0 wt % (red), 5 wt % (blue), 10 wt % (green), and 15 wt % (black), respectively.

respectively. They show characteristics similar to those of Li-PMMA solutions, although the absolute values of $\sigma'(\nu)$ are higher, and those of $\eta'(\nu)$ are lower than the corresponding values of the Li-PMMA solutions. The steady-state viscosity is determined by the slow dynamics of PMMA below 1 MHz, and the high-frequency edge of the relaxation associated with the slow dynamics of PMMA is observed on the low-frequency side. The high-frequency viscosity is increased by PMMA, and a relaxation of $\eta(\nu)$ appears in the 100 MHz region when the concentration of PMMA is 15 wt %. The ionic mobility is decoupled from the slow dynamics of PMMA, and it is reduced by the coupling with the structural relaxation in the 100 MHz region. Given that the observations above are common to Li-PMMA and TEA-PMMA, we can exclude the effects of strong Coulombic interaction specific to Li^+.

Figure 10 shows the relationship between the molar DC conductivity and the reciprocal viscosity of all the samples,

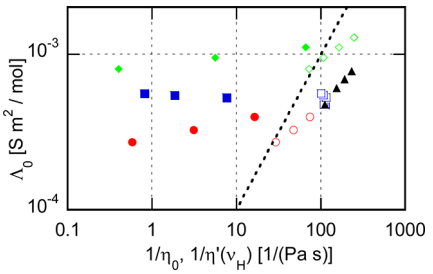

Figure 10. The molar DC conductivity, Λ_0, is correlated with the inverses of the steady-state shear viscosity, η_0 (filled symbols), or the real part of the high-frequency viscosity, $\eta'(\nu_H)$ (open symbols), where the value of ν_H is 100 MHz. The meanings of the symbols are, red circles for Li-PMMA, blue squares for Li-PEO, green diamonds for TEA-PMMA, and black triangles for Li-MIB, respectively. The dotted line, whose slope is unity, is the so-called the "ideal line" determined with aqueous KCl solution, which is shown as a guide for the eye.

which is called the "Walden plot". On the Walden plot, the Walden law is represented as straight lines whose slopes are unity. The Walden plot has been used to visualize the degree of coupling between the shear viscosity and ionic mobility.[4,37]

The correlation between Λ_0 and η_0 is weak in the cases of three polymer samples—Li-PMMA, Li-PEO, and TEA-PMMA systems—as was already demonstrated in Figure 1. On the other hand, the correlation between Λ_0 and η_0 is found in the mixed solvent of low molecular weight, PC and MIB, in harmony with the Walden law qualitatively. Closely looking at Figure 10, one may notice that the slope of the Li-MIB system, 0.7, is smaller than unity. In fact, there is no reason at present for the mobility of solute molecules as small as solvent ones to follow the hydrodynamic Stokes−Einstein relationship, which is a basis of the Walden law, and the deviations from the hydrodynamic theories as large as that of the present Li-MIB system have been reported in literatures.[38−40] A popular idea is to modify the hydrodynamic theory by replacing $1/\eta_0$ with $1/\eta_0^{\alpha}$, and one says that the mobility is determined by viscosity when the exponent α is sufficiently large, although it is smaller than unity. In this sense, we can say that the increase in Λ_0 with the addition of MIB is caused by the decrease in η_0. It is to be noted here that the fractional power dependence, $\propto 1/\eta_0^{\alpha}$, on shear viscosity was introduced empirically without theoretical bases. The fractional dependence nonetheless describes various experiments fairly well, and the value of α has been regarded as a measure of the strength of the coupling with shear viscosity.

Based on the idea that the microviscosity for the ionic mobility has something to do with the high-frequency viscosity, $\eta'(\nu_H)$ of polymer solutions at ν_H = 100 MHz is correlated with Λ_0 in Figure 10. The value of 100 MHz is chosen because it is sufficiently faster than slow polymer dynamics while slower than the structural relaxation in the 100 MHz region. Linear correlations are found for PMMA-based systems, while the

dx.doi.org/10.1021/jp4033172 | J. Phys. Chem. B XXXX, XXX, XXX−XXX

variations of both $\eta'(\nu_H)$ and Λ_0 of the Li-PEO system are quite small. The slopes of both the Li-PMMA and the TEA-PMMA systems are 0.4. Although the slope is smaller than that of Li-MIB system, we consider that the correlation between $\eta'(\nu_H)$ and Λ_0 of polymer gel electrolytes is comparable with that between viscosity and molecular mobility of nonpolymeric solutions, and the high-frequency viscosity, $\eta'(\nu_H)$, can be regarded as the so-called microviscosity for ionic mobility.

The relaxation spectra, $\eta(\nu)$ and $\sigma(\nu)$, show that both $\eta'(\nu_H)$ and Λ_0 are affected by the structural relaxation in the 100 MHz region, which we consider is the basis for the correlation between $\eta'(\nu_H)$ and Λ_0 demonstrated in Figure 10. However, it is still unclear whether the mechanism of the correlation between $\eta'(\nu_H)$ and Λ_0 found in this work is the same as that between η_0 and Λ_0 of nonpolymeric electrolytes, because the mechanism of the latter is yet to be resolved. Although computer simulation studies on supercooled liquids demonstrated that the Stokes−Einstein relationship between the self-diffusivity and shear viscosity of normal liquids is because these two properties are coupled to the same structural relaxation in cases of simple model liquids,[41,42] the examination of the same idea on realistic solute−solvent systems is not sufficient at present. Therefore, it will be required to clarify the microscopic origin of the Walden law of nonpolymeric electrolyte before the further pursuit of the establishment of the meanings of the microviscosity.

The concentration of polymers studied in this work is limited up to 15 wt % due to experimental reasons, while samples of higher polymer concentration are of practical importance. In particular, one can achieve solid polymer electrolyte by continuously reducing the amount of PC in the Li-PEO system. We have studied the transport properties of $LiClO_4$ dissolved in low molecular-weight PEO with experimental methods similar to those used in this work.[28] We demonstrated that the translational motion of ions is decoupled from the slow chain dynamics of polymer, and it is dominated by the segmental motion. We therefore consider that one of the conclusions of this work, that the ionic mobility is decoupled from the slow dynamics of polymers, holds at higher concentration of polymers. On the other hand, the meanings of the high-frequency viscosity would change at higher polymer concentration. Although it is regarded as the viscosity of low molecular-weight liquid around the polymer at low concentration, it should reflect the coupled motion of small molecules and polymer segments at higher polymer concentration.

5. CONCLUSION

We measured the frequency-dependent electric conductivity and shear viscosity of polymer gel electrolytes experimentally. The shear viscosity was determined by the dynamics of polymers whose characteristic frequency is below 1 MHz, while no dispersion of the conductivity was observed below 10 MHz. This means that the ionic mobility is completely decoupled from the slow dynamics of polymers, which explains the violation of the Walden law.

The dissolution of PMMA increased the high-frequency viscosity, $\eta'(\nu_H)$, while it decreased Λ_0. On the other hand, PEO barely affected both $\eta'(\nu_H)$ and Λ_0. A fairly good correlation was found between $\eta'(\nu_H)$ and Λ_0, as was demonstrated in Figure 10, which suggests that $\eta'(\nu_H)$ can be used as a probe of the so-called microviscosity defined in terms of ionic mobility.

A relaxation was found in both $\sigma(\nu)$ and $\eta(\nu)$ in the 100 MHz region in cases of PMMA-based solutions, and the relaxation frequency decreased with decreasing the concentration of PMMA. We assigned the relaxation to the structural relaxation of low molecular-weight electrolyte solutions between polymers. We consider that the correlation between $\eta'(\nu_H)$ and Λ_0 is because they are determined by the coupling between the same structural relaxation.

The idea of microviscosity is so convenient that it has been employed to explain dynamic properties in polymer gels in general, such as the translational and reorientational relaxation, motion of polymer, and reaction rates. We expect that its relationship with the high-frequency viscosity revealed in this work may be extended to the microviscosity for other properties.

AUTHOR INFORMATION

Corresponding Author

*E-mail: tyama@nuce.nagoya-u.ac.jp; Tel: +81-52-789-3592; Fax: +81-52-789-3273.

Notes

The authors declare no competing financial interest.

ACKNOWLEDGMENTS

This work was supported by JSPS KAKENHI Grant Numbers 22750012 and 24550019. T.Y. is also grateful to the Scholar Project of the Toyota Physical and Chemical Research Institute.

REFERENCES

(1) Feuillade, G.; Perche, Ph. Ion-conductive macromolecular gels and membranes for solid lithium cells. *J. Appl. Electrochem.* **1975**, *5*, 63−69.

(2) Stephan, A. M. Review on gel polymer electrolytes for lithium batteries. *Eur. Polym. J.* **2006**, *42*, 21−42.

(3) Bockris, J. O'M.; Reddy, A. K. N. *Modern Electrochemistry*; Plenum Press: New York, 1970, Vol. *1*.

(4) Angell, C. A.; Imrie, C. T.; Ingram, M. D. From Simple Electrolyte Solutions Through Polymer Electrolytes to Superionic Rubbers: Some Fundamental Considerations. *Polym. Int.* **1998**, *47*, 9−15.

(5) Svanberg, C.; Adebahr, J.; Ericson, H.; Börjesson, L.; Torell, L. M.; Scrosati, B. Diffusive and segmental dynamics in polymer gel electrolytes. *J. Chem. Phys.* **1999**, *111*, 11216−11221.

(6) Svanberg, C.; Bergman, R.; Börjesson, L.; Jacobsson, P. Diffusion of solvent/salt and segmental relaxation in polymer gel electrolytes. *Electrochim. Acta* **2001**, *46*, 1447−1451.

(7) Bohnke, O.; Frand, G.; Rezrazi, M.; Rousselot, C.; Truche, C. Fast ion transport in new lithium electrolytes gelled with PMMA. 1. Influence of polymer concentration. *Solid State Ionics* **1993**, *66*, 97−104.

(8) Park, U.-S.; Hong, Y.-J.; Oh, S. M. Fluorescence spectroscopy for local viscosity measurements in polyacrylonitrile (PAN)-based polymer gel electrolytes. *Electrochim. Acta* **1996**, *41*, 849.

(9) Sekhon, S. S. Conductivity behaviour of polymer gel electrolytes: Role of polymer. *Bull. Mater. Sci.* **2003**, *26*, 321−328.

(10) Saito, Y.; Okano, M.; Kubota, K.; Sakai, T.; Fujioka, J.; Kawakami, T. Evaluation of interactive effects on the ionic conduction properties of polymer gel electrolytes. *J. Phys. Chem. B* **2012**, *116*, 10089−10097.

(11) Funke, K.; Banhatti, R. D.; Brückner, S.; Cramer, C.; Krieger, C.; Mandanici, A.; Martiny, C.; Ross, I. Ionic motion in materials with disordered structures: conductivity spectra and the concept of mismatch and relaxation. *Phys. Chem. Chem. Phys.* **2012**, *4*, 3155−3167.

(12) Pas, S. J.; Banhatti, R. D.; Funke, K. Conductivity spectra and ion dynamics of a salt-in-polymer electrolyte. *Solid State Ionics* **2006**, *177*, 3135−3139.
(13) Šantić, A.; Wrobel, W.; Mutke, M.; Banhatti, R.; Funke, K. Frequency-dependent fluidity and conductivity of an ionic liquid. *Phys. Chem. Chem. Phys.* **2009**, *11*, 5930−5934.
(14) *Physical Acoustics*; Philippoff, W., Mason, W. P., Eds.; Academic Press: New York, 1965; Vol. *II*, Part B, Chapter 7.
(15) Schrag, J. L.; Stokich, T. M.; Strand, D. A.; Merchak, P. A.; Landry, C. J. T.; Radtke, D. R.; Man, V. F.; Lodge, T. P.; Morris, R. L.; Hermann, K. C.; Amelar, S.; Eastman, C. E.; Smeltzly, M. A. Local modification of solvent dynamics by polymeric solutes. *J. Non-Cryst. Solids* **1991**, *131*, 537−543.
(16) Lodge, T. P. Solvent dynamics, local friction, and the viscoelastic properties of polymer solutions. *J. Phys. Chem.* **1993**, *97*, 1480−1487.
(17) Peterson, S. C.; Echeverria, I.; Hahn, S. F.; Strand, D. A.; Schrag, J. L. Apparent relaxation-time spectrum cutoff in dilute polymer solutions: An effect of solvent dynamics. *J. Polym. Sci., Part B: Polym. Phys.* **2001**, *39*, 2860−2873.
(18) Morris, R. L.; Amelar, S.; Lodge, T. P. Solvent friction in polymer solutions and its relation to the high-frequency limiting viscosity. *J. Chem. Phys.* **1988**, *89*, 6523.
(19) Von Meerwall, E. D.; Amelar, S.; Smeltzly, M. A.; Lodge, T. P. Solvent and probe diffusion in aroclor solutions of polystyrene, polybutadiene, and polyisoprene. *Macromolecules* **1989**, *22*, 295.
(20) Bohnke, O.; Frand, G.; Rezrazi, M.; Rousselot, C.; Truche, C. Fast ion transport in new lithium electrolytes gelled with PMMA. 2. Influence of lithium salt concentration. *Solid State Ionics* **1993**, *66*, 105−112.
(21) Yamaguchi, T.; Hayakawa, M.; Matsuoka, T.; Koda, S. Electric and mechanical relaxations of $LiClO_4$-propylene carbonate systems in 100 MHz region. *J. Phys. Chem. B* **2009**, *113*, 11988−11998.
(22) Hayamizu, K.; Aihara, Y.; Price, W. S. Correlating the NMR self-diffusion and relaxation measurements with ionic conductivity in polymer electrolytes composed of cross-linked poly(ethylene oxide-propylene oxide) doped with $LiN(SO_2CF_3)_2$. *J. Chem. Phys.* **2000**, *113*, 4785−4793.
(23) Hayamizu, K.; Sugimoto, K.; Akiba, E.; Aihara, Y.; Bando, T.; Price, W. S. An NMR and ionic conductivity study of ion dynamics in liquid poly(ethylene oxide)-based electrolytes doped with $LiN(SO_2CF_3)_2$. *J. Phys. Chem. B* **2002**, *106*, 547−554.
(24) Hayamizu, K.; Akiba, E.; Bando, T.; Aihara, Y.; Price, W. S. NMR studies on poly(ethylene oxide)-based polymer electrolytes with different cross-linking doped with $LiN(SO_2CF_3)_2$. Restricted diffusion of the polymer and lithium ion and time-dependent diffusion of the anion. *Macromolecules* **2003**, *36*, 2785−2792.
(25) Masuda, A.; Ushida, K.; Nishimura, G.; Kinjo, M.; Tamura, M.; Koshino, H.; Yamashita, K.; Kluge, T. Experimental evidence of distance-dependent diffusion coefficients of a globular protein observed in polymer aqueous solution forming a network structure on nanometer scale. *J. Chem. Phys.* **2004**, *121*, 10787−10793.
(26) Masuda, A.; Ushida, K.; Okamoto, T. New fluorescence correlation spectroscopy (FCS) suitable for the observation of anomalous diffusion in polymer solution: Time and space dependences of diffusion coefficients. *J. Photochem. Photobiol. A* **2006**, *183*, 304−308.
(27) Casieri, C.; Monaco, A.; De Luca, F. Evidence of temperature-induced subdiffusion of water on the micrometer scale in a nafion membrane. *Macromolecules* **2010**, *43*, 638−642.
(28) Yamaguchi, T.; Yamada, Y.; Koda, S. Shear and conductivity relaxations of lithium ion electrolytes in polyethyleneglycol dimethyl ethers. *J. Mol. Liq.* **2012**, *172*, 93−101.
(29) Buchner, R.; Hefter, G. T.; May, P. M. Dielectric relaxation of aqueous NaCl solutions. *J. Phys. Chem. A* **1999**, *103*, 1−9.
(30) Wei, Y.-Z.; Sridhar, S. Radiation-corrected open-ended coax line technique for dielectric measurements of liquids up to 20 GHz. *IEEE Trans. Microwave Theory Tech.* **1991**, *39*, 526−531.
(31) Barthel, J.; Buchner, R.; Hölzl, G.; Münsterer, M. Dynamics of benzonitrile, propylene carbonate and butylene carbonate: The influence of molecular shape and flexibility on the dielectric relaxation behaviour of dipolar aprotic liquids. *Z. Phys. Chem.* **2000**, *214*, 1213−1231.
(32) Yamaguchi, T.; Mikawa, K.; Koda, S. Shear relaxation of water-ionic liquid mixtures. *Bull. Chem. Soc. Jpn.* **2012**, *85*, 701−705.
(33) Behrends, R.; Kaatze, U. A high frequency shear wave impedance spectrometer for low viscosity liquids. *Meas. Sci. Technol.* **2001**, *12*, 519−524.
(34) Sharma, J. P.; Sekhon, S. S. PMMA-based polymer gel electrolytes containing NH_4PF_6: Role of molecular weight of polymer. *Mater. Sci. Eng., B* **2006**, *129*, 104−108.
(35) Deepa, M.; Agnihotry, S. A.; Gupta, D.; Chandra, R. Ion-pairing effects and ion−solvent−polymer interactions in $LiN(CF_3SO_2)_2$−PC−PMMA electrolytes: A FTIR study. *Electrochim. Acta* **2004**, *49*, 373−383.
(36) Kumar, R.; Sekhon, S. S. Evidence of ion pair breaking by dispersed polymer in polymer gel electrolytes. *Ionics* **2004**, *10*, 436−442.
(37) Xu, W.; Cooper, E. I.; Angell, C. A. Ionic liquids: Ion mobilities, glass temperatures, and fragilities. *J. Phys. Chem. B* **2003**, *107*, 6170−6178.
(38) Evans, D. F.; Tominaga, T.; Davis, H. T. Tracer diffusion in polyatomic liquids. *J. Chem. Phys.* **1981**, *74*, 1298−1305.
(39) Tominaga, T.; Matsumoto, S. Diffusion of polar and nonpolar molecules in water and ethanol. *Bull. Chem. Soc. Jpn.* **1990**, *63*, 533−537.
(40) Kowert, B. A.; Watson, M. B. Diffusion of organic solutes in squalane. *J. Phys. Chem. B* **2011**, *115*, 9687−9694.
(41) Zangi, R.; Kaufman, L. J. Frequency-dependent Stokes−Einstein relation in supercooled liquids. *Phys. Rev. E* **2007**, *75*, 051501.
(42) Kim, K.; Saito, S. Role of the lifetime of dynamical heterogeneity in the frequency-dependent Stokes−Einstein relation of supercooled liquids. *J. Phys. Soc. Jpn.* **2010**, *79*, 093601.